

AMERICAN UNIVERSITY OF BEIRUT

PARTICLE IMAGE VELOCIMETRY OF HIGH INTENSITY
FOCUSED ULTRASOUND (HIFU) FIELD

by
HUSSEIN SA'ID DAOUD

A thesis
submitted in partial fulfillment of the requirements
for the degree of Master of Engineering
to the Department of Mechanical Engineering
of the Faculty of Engineering and Architecture
at the American University of Beirut

Beirut, Lebanon
September 2015

AMERICAN UNIVERSITY OF BEIRUT

PARTICLE IMAGE VELOCIMETRY OF HIGH INTENSITY
FOCUSED ULTRASOUND (HIFU) FIELD

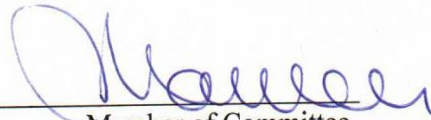
by
HUSSEIN SA'ID DAUD

Approved by:



Advisor

Dr. Ghanem Oweis, Associate Professor
Department of Mechanical Engineering



Member of Committee

Dr. Marwan Darwish, Professor
Department of Mechanical Engineering



Member of Committee

Dr. Ghassan Antar, Associate Professor
Department of Physics

Date of thesis defense: September 15, 2015

AMERICAN UNIVERSITY OF BEIRUT

THESIS, DISSERTATION, PROJECT RELEASE FORM

Student Name: _____

Last

First

Middle

Master's Thesis

Master's Project

Doctoral Dissertation

I authorize the American University of Beirut to: (a) reproduce hard or electronic copies of my thesis, dissertation, or project; (b) include such copies in the archives and digital repositories of the University; and (c) make freely available such copies to third parties for research or educational purposes.

I authorize the American University of Beirut, **three years after the date of submitting my thesis, dissertation, or project**, to: (a) reproduce hard or electronic copies of it; (b) include such copies in the archives and digital repositories of the University; and (c) make freely available such copies to third parties for research or educational purposes.

Signature

Date

ACKNOWLEDGMENTS

I would like to thank all the people that supported and helped me in the past two years. Without them, I wouldn't finish this thesis.

I thank my advisor Dr. Ghanem Oweis for his continuous support and guiding me throughout my master. Moreover, I want to extend my gratitude to the committee members: Dr. Ghassan Antar and Dr. Marwan Darwish.

Thanks to all my friends and colleagues in AUB. Thanks to my friends in the fluids lab Mhamad Mahdi Alloush, Adnan El Makdah, and Moath Al Qraini.

Lastly and most importantly, thanks to my entire family who was beside me every minute of my study years. My father and my mother, thank you for raising, supporting and teaching me. To you I dedicate my thesis.

ABSTRACT OF THE THESIS OF

Hussein Sa'id Daoud for Master of Engineering
Major: Mechanical Engineering

Title: Particle Image Velocimetry of High Intensity Focused Ultrasound (HIFU) Field

High Intensity Focused Ultrasound (HIFU) is one of thermal ablation techniques that are used to treat the cancer tumors by generating coagulation necrosis in the tumor cells. It is designed to focus a high acoustic intensity at a precisely defined location called Focal Spot leading to increase temperature at this spot to a degree that is sufficient to ablate the cancerous biological tissues. Prostate, renal, bladder, and testicular tumors are examples for the tumors that have been treated with HIFU.

Despite its use, until now there is no international standard that accurately describes the field induced by the HIFU. Particle Image Velocimetry (PIV), on the other hand, provides a non-intrusive technique to measure and characterize the fluid flow. It was used in many previous works to measure the Acoustic Particle Velocity of low-frequency sound fields.

In this work, a novel PIV procedure that is appropriate for using in high-frequency applications will be introduced. This procedure will be used to investigate a HIFU field that arises in a water bath at and around the focal spot. Moreover, the influence of changing the HIFU intensity on the resulting acoustic particle velocity field will be measured to estimate the availability of using PIV as a calibration tool for the HIFU transducers.

CONTENTS

ACKNOWLEDGMENTS.....	v
ABSTRACT	vi
ILLUSTRATIONS	ix
Chapter	
I. INTRODUCTION.....	1
A. Background.....	2
1. Waves.....	2
2. Sound Waves in Fluids	4
3. Acoustic Velocimetry.....	5
4. Ultrasound Transducers	7
5. High Intensity Focused Ultrasound (HIFU).....	8
B. Problem Statement.....	10
II. SYSTEM SETUP	12
A. Water Bath.....	12
B. Laser, Camera, Delay Generator System.....	12
C. HIFU Transducer	14
III. PRELIMINARY EXPERIMENT	16
A. Procedure Description	16

B. Results	17
C. Conclusions from the Preliminary Experiment	21
IV. PROPOSED PROCEDURE.....	22
A. Procedure Description	22
B. Matlab Simulation	23
C. Real-World Experiment.....	27
V. ACOUSTO-OPTICS MEASUREMENT TECHNIQUE.....	34
A. Procedure Description	34
B. Distance Effect	36
C. Input Power Effect.....	38
D. Proposed Calibration Procedure	43
VI. CONCLUSION.....	45
REFERENCES.....	46
Appendix	
1. TIME SCHEME FOR PIV SETS IN THE PIV BLOCKS EXPERIMENT.....	48
2. TIME SCHEME FOR PIV SETS IN THE ACOUSTO- OPTICAL EXPERIMENT.....	51

ILLUSTRATIONS

Figure	Page
1. A schematic of PIV system setup	13
2. Intensity about focus, Fundamental frequency, Zero reference is 51.712 mm beyond exit plane. Positive direction is away from exit plane.	14
3. Efficiency measurements at 497.5 kHz (fundamental best match) averaged 75%. Efficiency measurements at 1,640 kHz (third harmonic best match) averaged 57% [1].....	15
4. A schematic of the scenario of the preliminary experiment	17
5. Velocity Vector distribution on a plane	18
6. Displacement vector at different inter-frame time (time is in nsec)	19
7. dx/dt vector at different inter-frame timings when the amplifier supplies its maximum amplification and the function generator supplies (a) 1Vpp (b) 4Vpp (c) the difference between them.....	20
8. Time block for the proposed experiment.....	23
9. Sensitivity of the RMS- velocity value with the increment time.....	24
10. Velocity fields resulted from Matlab simulation of PIV blocks procedure at three different times, $\tau=100$ ns.....	25
11. The expected time-velocity profile at three different points in the field resulting from Matlab simulation	26
12. The RMS-velocity field resulted from Matlab simulation.....	27
13. Time scheme of first and second PIV blocks	29
14. First PIV block fields; (a) the average displacement field for set 1, (a) the average displacement field for set 2, (c) the displacement field for PIV block 1.	30

15.	Time-velocity profile at three points in the field	31
16.	Time RMS average velocity field at focal point resulted from applying PIV block technique	32
17.	Acousto-optical effect as appears on capturing pictures for grid paper placed at HIFU field.....	35
18.	Spatial RMS average deformation rate of grids under the effect of HIFU field at different radial distances	37
19.	Changing of the acousto-optical effect with distance of grid sheet from the HIFU axis.....	38
20.	Time scheme for acousto-optical experiment	39
21.	The time-average deformation rate fields at five different powers.....	41
22.	Time and spatial averaged velocity distribution along the transverse direction around the HIFU focal spot	42
23.	The change of the time-spatial RMS average deformation rate along HIFU axis with the change of acoustic intensity.....	43

CHAPTER I

INTRODUCTION

Unlike the common Ultrasound transducers which are used as diagnostic tools, *High Intensity Focused Ultrasound (HIFU)* is a therapeutic tool. It is designed to focus a high acoustic intensity at a precisely defined location called Focal Spot leading to increase temperature at this spot to a degree that is sufficient to ablate the cancerous biological tissues. Prostate, renal, bladder, and testicular tumors are examples for the tumors that have been treated with HIFU.

Until now there is no international standard that accurately describes the field induced by the HIFU. The interruption of the field and the damage of sensors are the most important problems associated with using the *Hydrophone* measurement (which is currently the most widely used tool) to characterize the HIFU field. These problems are associated with using any of the intrusive techniques.

Particle Image Velocimetry (PIV), on the other hand, provides a non-intrusive technique to measure and characterize the fluid flow. It was used in many previous works to measure the Acoustic Particle Velocity of low-frequency sound fields. However, the very short wavelength in the cases of High-frequency ultrasound sources make the typical PIV procedure inconvenient to study the fields induced by this type of transducers.

In this work, a novel PIV procedure that is appropriate for using in high-frequency applications will be introduced. This procedure will be used to investigate a HIFU field that arises in a water bath at and around the focal spot. Moreover, the influence of changing the HIFU intensity on the resulting APV field will be measured to introduce the PIV as a valid calibration tool for the HIFU transducers.

A. Background

In this section the concept, classifications, and equations of waves will be presented. Then, the special interest will be taken on the propagation of sound waves in a fluidic medium. The concepts of acoustic particle velocity, sound pressure, and sound Intensity and the relations among each other will be clarified. At the end, HIFU concept, applications, and the techniques for characterizing its field will be presented.

I. Waves

A wave is an oscillation accompanied by a transfer of energy that travels through space or mass. Based on their nature, the waves are classified into two main types: *Mechanical Waves* and *Electromagnetic Waves*. Mechanical waves propagate through a medium, and the substance of this medium is deformed. Electromagnetic waves do not require a medium. Instead, they consist of periodic oscillations of electrical and magnetic fields generated by charged particles

The waves are divided base on the method of propagation into *Longitudinal Waves* and *Transverse Waves*. In the longitudinal type, the waves propagate in the same direction

of displacement for the medium's particles. In the transverse form, the wave propagate orthogonally (at right angles) to the direction of displacement for the medium's particles.

Another important division is based on the wave front geometry. In a *Planar Wave* the wave front is located on a plane that propagates in space, while a *Circular Wave* propagates symmetrically around a reference point (as a sphere or a ring), or around a reference line (as a cylinder). {15 Azhari, Haim 2010}

a. Wave Function

Generally speaking, a wave propagating along the positive direction of the X axis can be described by the general function ($U(x, t) = U(x - ct)$), whereas a wave propagating along the negative direction of the X axis can be described by ($U(x, t) = U(x + ct)$).

The wave equation for the one dimensional wave propagates in a homogeneous medium is given by equation (1), the corresponding wave equation in the three dimensional case is given by equation (2)

$$\frac{\partial^2 U}{\partial x^2} = \frac{1}{c^2} \cdot \frac{\partial^2 U}{\partial t^2} \quad (1)$$

$$\nabla^2 U = \frac{1}{c^2} \cdot \frac{\partial^2 U}{\partial t^2} \quad (2)$$

The most basic wave is the spatially one-dimensional sine wave with amplitude A described by the equation:

$$U(x, t) = A \sin\left(\frac{2\pi}{\lambda} x - 2\pi f t + \phi\right) \quad (3)$$

Where U can be any of alternating parameter of the wave, in the case of sound wave, it can be the acoustic pressure or acoustic particle velocity. A is the maximum

amplitude of U . λ is the wavelength, which is defined as the distance traveled by one cycle propagating away from the source. f is the frequency, which is defined as the number of complete cycles per unit of time. ϕ is the phase constant.

The other related important parameters are the period and the wave velocity. The period of the wave T is the time required to complete one cycle; it is the reciprocal of the frequency ($T = 1/f$). The velocity (c) is the speed of propagating of the wave. The relation between the frequency, wavelength, and the speed of wave is given by ($\lambda = c/f$).

2. *Sound Waves in Fluids*

Let's assume a fluid element that exists in rest at (x_0, y_0, z_0) has an equilibrium pressure and density of P_0 and ρ_0 respectively. When a sound wave pass through this element, the instantaneous pressure of the element will change. This led to define the concept of *Acoustic Pressure* which is the difference between the instantaneous pressure and the rest pressure.

$$p = P - P_0 \quad (4)$$

this pressure will be different at each point in the field at any given time point, which means that there is always a pressure gradient in the field, the fluid element will response to this pressure gradient by moving from its original location having *Acoustic Particle Displacement and Velocity*.

Because both the acoustic pressure and the acoustic velocity change periodically with time, the *RMS values* are used to describe them and these RMS values are related in by the following relation { { 16 Rockliff, Dawn 2002 } } :

$$p_{rms} = \rho_0 c u_{rms} \quad (5)$$

Another important concept associated with the propagation of ultrasound wave through a fluid is the *Acoustic Intensity*, which quantify the average rate of energy transmitted through a unit area. It is related to the acoustic pressure and acoustic velocity by the following equation, Where T is the time of one complete cycle:

$$I = \frac{1}{T} \int_0^T p u dt \quad (6)$$

It is conventional to describe the intensity in term of decibels with respect to reference value I_{ref} instead of the absolute value; the decibel value can be obtained using the following relation {{16 Rockliff, Dawn 2002}}:

$$Intensity Level (dB) = 10 \log\left(\frac{I}{I_{ref}}\right) \quad (7)$$

The specific impedance is defined as the ratio of the acoustic pressure to acoustic particle velocity

$$z = \frac{p}{u} \quad (8)$$

For a plane wave

$$z = \pm \rho_0 c \quad (9)$$

3. *Acoustic Velocimetry*

The techniques used to measure acoustic velocity in a sound field are classified into: {{1 Tonddast-Navaei, Ali 2006; 16 Rockliff, Dawn 2002}}

a. Intrusive Techniques

Rayleigh disc technique uses a suspended disc in a fluid. When a sound field is applied on the fluid, the field exerts a torque on the disc producing a deviation from its equilibrium position. The device cannot measure flow direction, requires many corrections, and its size considered bulk for many applications. This old technique is no longer in use.

In A *two-microphone* method, two closely spaced microphones are placed in the sound field to measure the pressure gradient in the field, acoustic velocity can be calculated then using equations of motions.

Hot-Wire Anemometry (HWA) is another flow measuring techniques that was used to measure the acoustic velocity. It consists of a thin wired sensor soldered between two needles and it acts as one of the arms of a Wheatstone bridge. A heating electric current is applied on the sensor. And the cooling effect due to the convection is used to measure the fluid velocity.

The *Microflown* is based on a thermo-electric structure, is convenient to use but has an upper limit for velocity measurement which is usually lower than the range of interest in acoustic studies.

Because of their physical presence in a sound field, and because their dimensions are not negligible when compared to the wavelength of the sound field, all of the devices used in the techniques mentioned so far have the disadvantage of being intrusive in nature.

b. Non-Intrusive Techniques

In the *Laser Doppler Velocimetry*, tracer particles were added to the fluid. By measuring the *Doppler shift* of the frequency between the incidents waves and reflected

waves from tracer particles, the velocity of the fluid can be predicted. The problem of this technique is that it is a point technique, which means that it should be repeated many times at different locations to provide a whole field measurement.

Particle Image Velocimetry (PIV) is a non-invasive, instantaneous, whole field velocity measurement tool. In the PIV measurement, a minute-trace particles are added to the fluid flow and they are illuminated twice using Laser source in a short time interval. The reflected light from the particles is recorded by camera in a single or multiple frames. The frames are then analyzed by special software to determine the displacement of the tracer particles.

Hann and Greated suggest a novel PIV method to measure the acoustic particle velocity and mean flow velocity when both a fluid flow and acoustic field are present. However, they apply this method to measure a field of standing wave has a frequency in the range of 1.6 KHz which is much lower than a range of HIFU {{18 Hann, DB 1997; 19 Hann, DB 1997}}.

Many other works used PIV to study the acoustic particle velocity. However all of them were for relatively low-frequency applications. {{11 Berson, Arganthaël 2008; 2 Fischer, André´ 2008; 8 Humphreys, William M 1998}}

4. *Ultrasound Transducers*

The term transducer, in general, refers to a device that converts energy from one form to another. In the case of ultrasound transducer, the types of energy of interest are electrical oscillation and acoustic vibration.

Nowadays, almost all medical ultrasound transducers are made of piezoelectric crystals, where a piezoelectric material is a material that deformed under the action of applying voltage across its surfaces. Moreover, when it deforms, a voltage difference appears between its opposite surfaces. Depending on this property, if AC current applied to piezoelectric crystal at its resonance frequency, it will vibrate at this frequency generating a periodic change in the pressure of the fluid around the crystal surface.

5. *High Intensity Focused Ultrasound (HIFU)*

HIFU is one of thermal ablation techniques that are used to treat the cancer tumors by generating coagulation necrosis in the tumor cells. HIFU achieves that by focusing a very high acoustic intensity ($100\text{-}10\,000\text{ W/cm}^2$) in a very small region called focal point. It has been clinically applied to treat prostate, pancreas, liver, breast, and uterine tumors. More than 100 000 cases have been benefited from HIFU treatment, most of them are from Asia and Europe.{{22 Zhou,Y.F. 2011}}

The advantages that HIFU provides in comparison to the other cancer treatment techniques are: "pain is minimized (the procedure is minimally- or non-invasive); the procedure cost is low as compared with traditional surgery; there are no remaining scars; recovery is faster than with traditional surgical methods; if any hemorrhage occurs, ultrasound (US) has the potential to stop the bleeding; the therapy can be repeated, theoretically, an infinite number of times because there is no dose limit; there is no ionizing radiation from magnetic resonance imaging (MRI) and diagnostic US, as opposed to other

systems that are guided by X-rays; and maintenance of the system is low." {{22 Zhou,Y.F. 2011}}

HIFU transducer can be a single element with a concave shape, multi-elements on a concave shape surface, or even a flat transducer with acoustic lenses. Changing the ablation area of a transducer, to cover the whole volume of the tumor, can be performed by mechanically moving or rotating the transducer. In the case of multi-elements transducer, changing the ablation area can be performed without moving the transducer itself by the mean of phase shift technology, in which the focus point of the transducer moved by adjust the amplitude and the phase of each element individually.

a. Characterization of HIFU Field

One of the procedures that were described by the literature is done using a hydrophone and a radiation force balance. First, a hydrophone is used to scan across the focal plane of the HIFU transducer to determine the focal cross-sectional area of the HIFU beam. Then, the radiation force balance is used to measure the output acoustic power. By dividing the acoustic power over the cross sectional area, the spatially averaged intensity (I_{SAL}) of the transducer is obtained. {{20 Canney, Michael S 2008}}

Another attempt to characterize the HIFU field was done using infrared camera to measure the temperature rises in a thin absorber located at HIFU field. This temperature rise was used then to estimate the HIFU intensity distribution by using two different method; the first one based on assuming a linear relation between the temperature rise and the free field intensity. While the second depended in build a correlation between infrared

measured temperature, calculated temperature from a model used heat equation, and the free field HIFU intensity.{{7 Shaw, A 2011}}

b. Lack of Standard to Measure HIFU:

The importance of the attempts to characterize the HIFU field s stems from the agreement among the literatures that there is a lack an approved characterization until now. The following quotes from relatively recent publications show that:

- 1- “For clinically relevant high powers, there are no alternative measurement standards available to accurately characterize medical ultrasound fields generated by HIFU transducers.”{{4 Hariharan, Prasanna 2008}}
- 2- HIFU is a very new application and our understanding of how best to calibrate systems is at an early stage. There are currently no accepted international standards for the calibration of HIFU systems.{{6 Shaw, Adam 2008}}
- 3- “Despite the fact that the HIFU systems are already in clinical use, until now there have been no international standards published for the accurate description of the fields created by them “{{21 Bessonova, Olga V 2013}}

B. Problem Statement

In this experiment, PIV is used to investigate a HIFU field that arises in a water bath at and around the focal spot. The influence of changing the HIFU intensity on the resulting velocity field will be determined. Moreover, the nature of the particle movement in response to the ultrasound wave will be characterized.

As we want to find an alternative tool for measure the HIFU field other than the currently used hydrophone, this alternative tool must provide the same aspects of the data that can be measured by the hydrophone and get rid of the limitation of it; the hydrophone provides an RMS value for the pressure measurements taken with time for a specific point in space. So, the alternative tool must provide the RMS of the values measured by periodic time for the same point in space. Nonetheless, the alternative tool must be non-invasive to avoid the interruption of the HIFU field. In this work we aim to:

- 1- Perform typical PIV procedure to measure the acoustic particle velocity at the focal point of the HIFU to specify the features and the limitations of this procedure.
- 2- Propose a new PIV procedure to measure the acoustic particle velocity for the HIFU field that avoids the limitations of the typical procedure
- 3- Propose an optical and non-intrusive technique can be used by the HIFU manufacturers to calibrate their transducers.

CHAPTER II

SYSTEM SETUP

A schematic of the Acoustic Particle velocimetry system is shown in Figure 1. It is similar to a system used by Quraini et al to measure the acoustic streaming {{24 Quraini, Moath Mustafa 2012}}. The laser source and the camera were programmed to acquire two separate image frames (an image pair) at a controllable inter-frame time. The image pairs are processed with the PIVLAB Matlab software, developed by {{23 Han, Donghee 2003}}, producing an acoustic velocity field from each pair. The components of the system are as follows:

A. Water Bath

The HIFU transducer was placed in a water-filled cast acrylic tank measuring $20 \times 20 \times 25 \text{ cm}^3$ with a 1.2 cm thick wall. The HIFU transducer was mounted in the side wall of the tank. Before launching the experiments, the tank was filled with distilled and deaerated water. Titanium dioxide nano-particles (100 nm, catalog number 677469, Sigma Aldrich, St. Louis, MO) were added as flow tracers to a water vial. This vial was located at the focal region of the HIFU.

B. Laser, Camera, Delay Generator System

Dual-head Nd:YAG laser (model Quantel, Big Sky, Montana, USA) was used with a system of lenses and mirrors to produce a very thin laser sheet cutting the field

longitudinally (parallel to the acoustic beam axis) and illuminating the trace- particles at and around the focal point. The camera (model SensiCam, PCO, Germany) was operated at PIV mode which allows the camera to take two frames for the tracer particles at a time controlled by the delay generator.

A delay generator (model DG100N, Thorlabs, NJ) was used to control the system. First, it triggered the HIFU transducer to produce the ultrasound waves. Then, it triggered the camera and the laser simultaneously twice to capture the two frames.

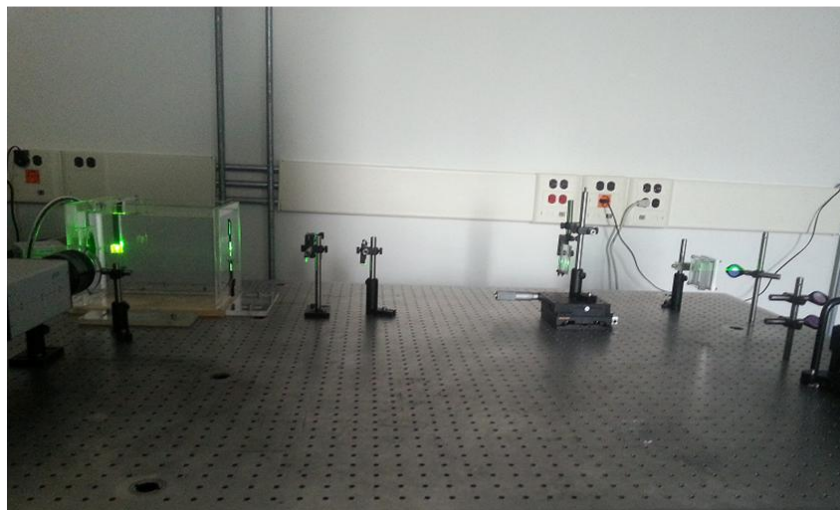
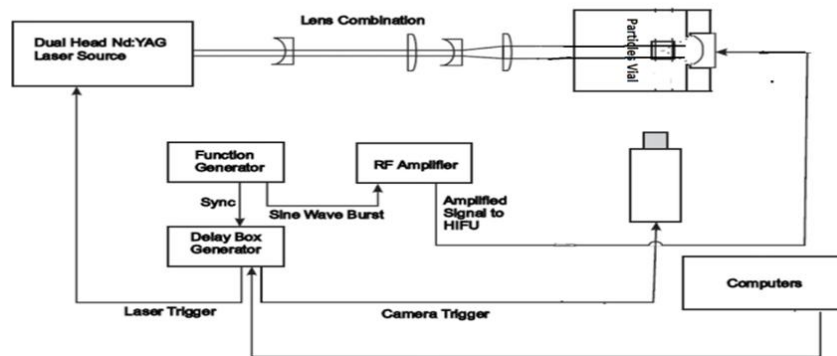


Figure 1: A schematic of PIV system setup

C. HIFU Transducer

The HIFU transducer was a single element piezo-ceramic transducer (model H-107, Sonic Concept) with a 64 mm diameter, 62.7 mm focal length. It can be operated at fundamental frequency of 0.5 MHz or at third harmonic frequency of 1.6 MHz. Figure 2 shows its intensity distribution around the focal point. The average of its power conversion efficiency, regarding to the manufacturer tests, are 75% & 57% at the fundamental and the third harmonic frequencies respectively (Figure 3).

It was operated at burst mode of 1 ms and frequency of 500 KHz using a function generator (model 33252A, Agilent Tech. Inc., CA, USA) and a radiofrequency amplifier (model A75, Amplifier Research, IL, USA). The fundamental frequency (500 KHz) was chosen during the experiments because it has longer wavelength than the third harmonic frequency which makes the measurement easier.

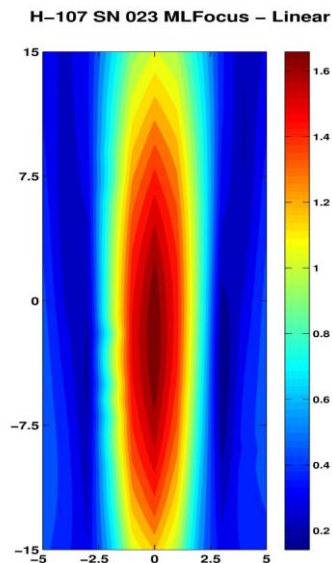
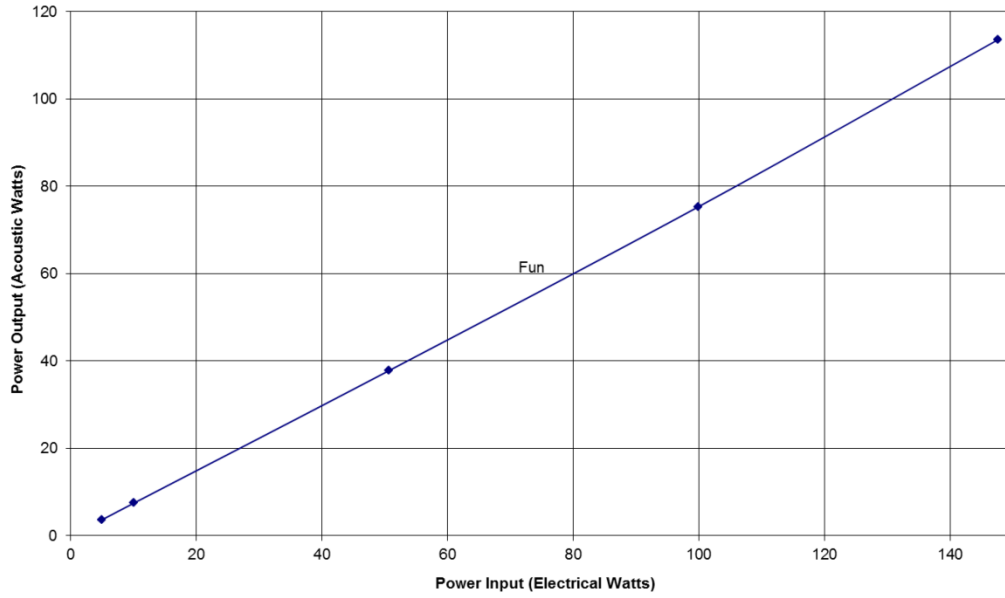


Figure 2: Intensity about focus, Fundamental frequency, Zero reference is 51.712 mm beyond exit plane. Positive direction is away from exit plane.

H-107 S/N 023 Power Linearity
Fundamental Best Match (497.5 kHz)



H-107 S/N 023 Power Linearity
Third Harmonic Best Match (1,640 kHz)

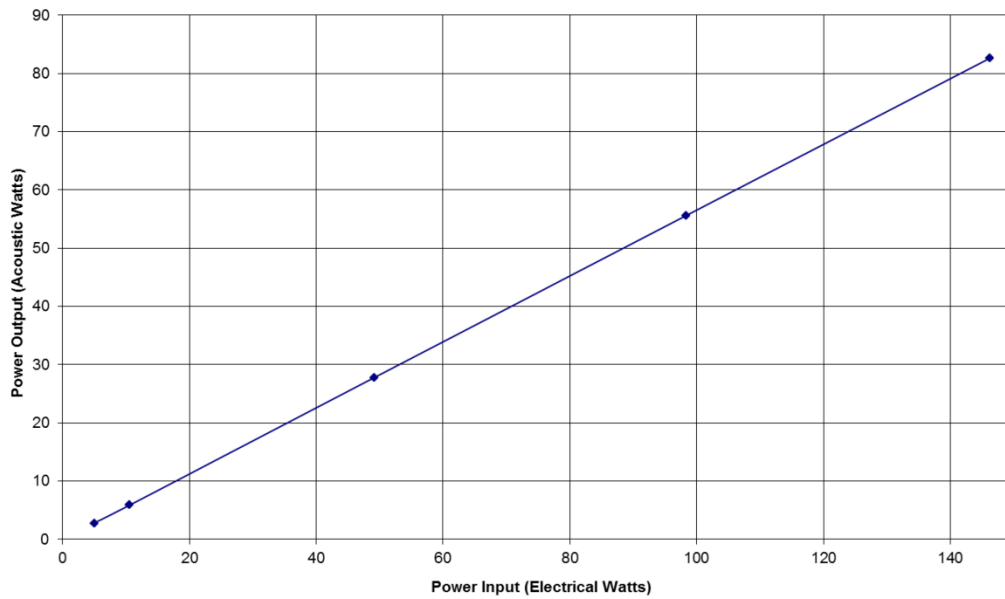


Figure 3: Efficiency measurements at 497.5 kHz (fundamental best match) averaged 75%. Efficiency measurements at 1,640 kHz (third harmonic best match) averaged 57% [1]

CHARTER III

PRELIMINARY EXPERIMENT

A. Procedure Description

In this experiment, the PIV was performed using pictures captured at $t=T-\tau/2$ & $t=T+\tau/2$ from the HIFU-trigger time, where T is the time between the HIFU pulse starting and the center time between the two PIV frames, and τ is the inter-frame time (figure 4). The experiments were performed using 7 different inter-frame time (τ) values ranging between 500- 2000 ns with an increment of 250 ns. In each case, 110 PIV pairs were captured to get the average of them. A delay interval of 1 s was applied between consecutive HIFU bursts.

Two different powers were used. In each of them, the maximum amplification power is used, but the applied voltage from the function generator was 1 V_{pp} in one of them and 4 V_{pp} in the other. A complete PIV set was taken from each power, where each set had PIV measurements at all increments of τ . Moreover, the experiment was repeated at three different camera views: wide view 30*22 mm which covers 8 acoustic waves in a camera frame, narrow view 12*10 mm which covers 3 acoustic waves, and single wave view 5*4 mm.

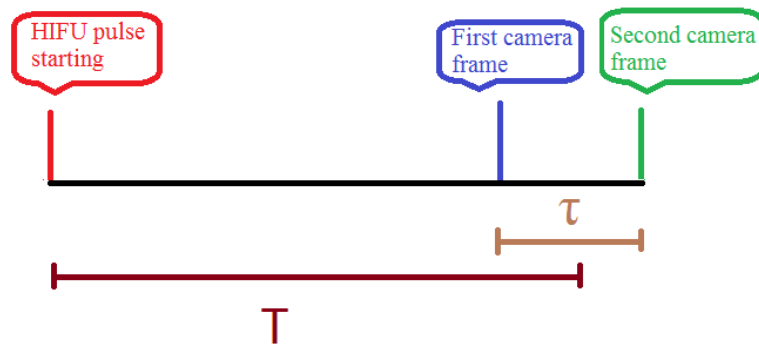


Figure 4: A schematic of the scenario of the preliminary experiment

B. Results

Figure 5 represents the Acoustic Particles Velocity field on the plane of the camera frame where the length of a row represents its velocity. The periodic change of the pressure is evident since the particles moves from the higher pressure regions to the lower pressure ones. Moreover, the longitudinal components of the velocity vectors (x-component) are shown to be dominant. The considerable increase in the velocity amplitude in a specific region indicates the focal spot.

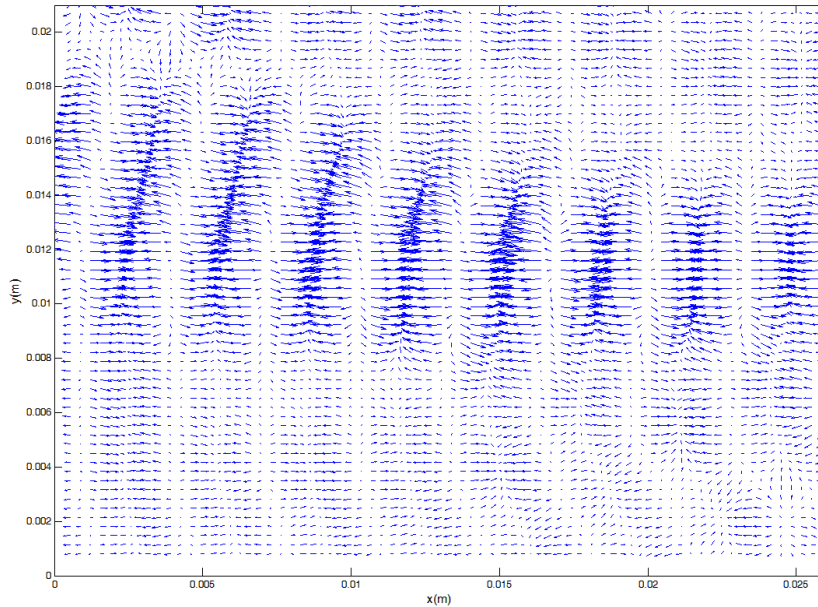


Figure 5 Velocity Vector distribution on a plane

Figure 6 shows the displacement vector at the focal point at different inter-frame intervals (τ). One can notice that the amplitude of displacement increases when τ increases and reaches a maximum at $\tau=1000\text{ns}$ (which represent the half of the wave length of the ultrasound). Then it starts to decrease until reaching a minimum at $\tau=2000\text{ns}$. This phenomenon occurs due to the nature of the particles' movement. In reality, the particle moves in a back and forth oscillatory motion. The maximum displacement occurs at half the wavelength, and then the particle starts to go back until it reaches its original position at the end of the cycle. Furthermore, all displacement vectors shown in Figure 6 are in-phase with each other. This is because the center time between the two frames for each pair was kept constant (T) with respect to the start time of the HIFU exposure.

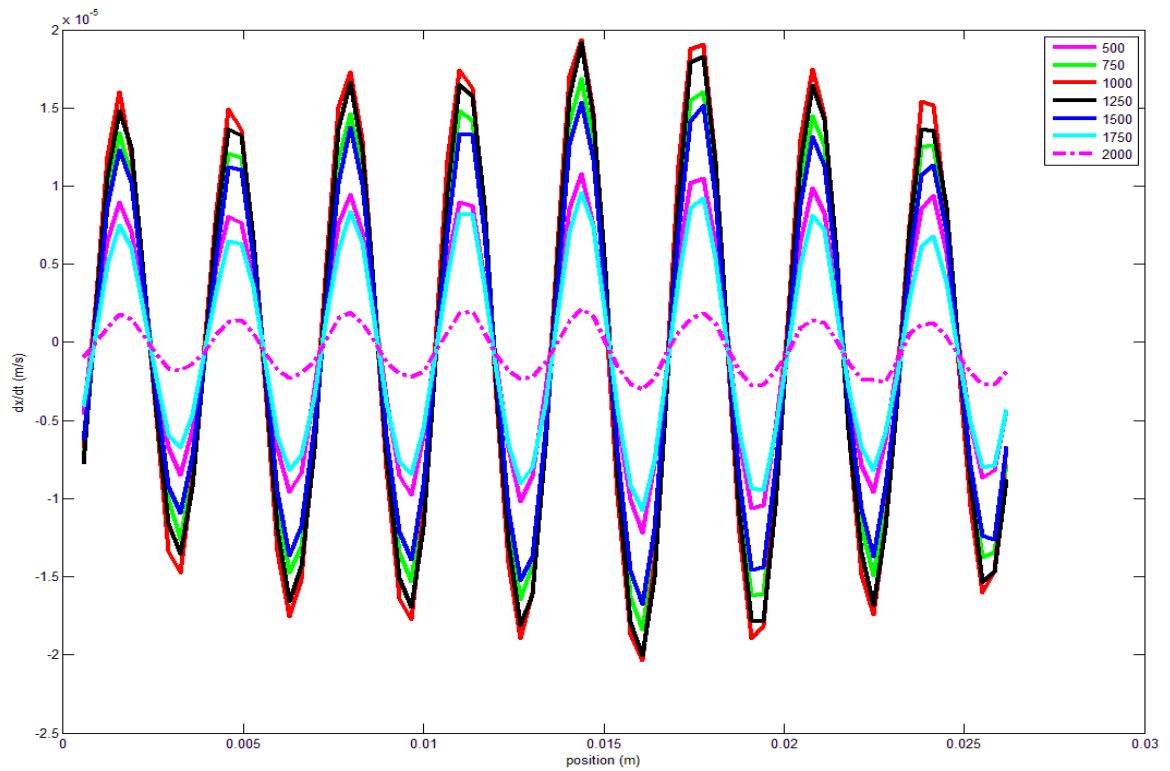
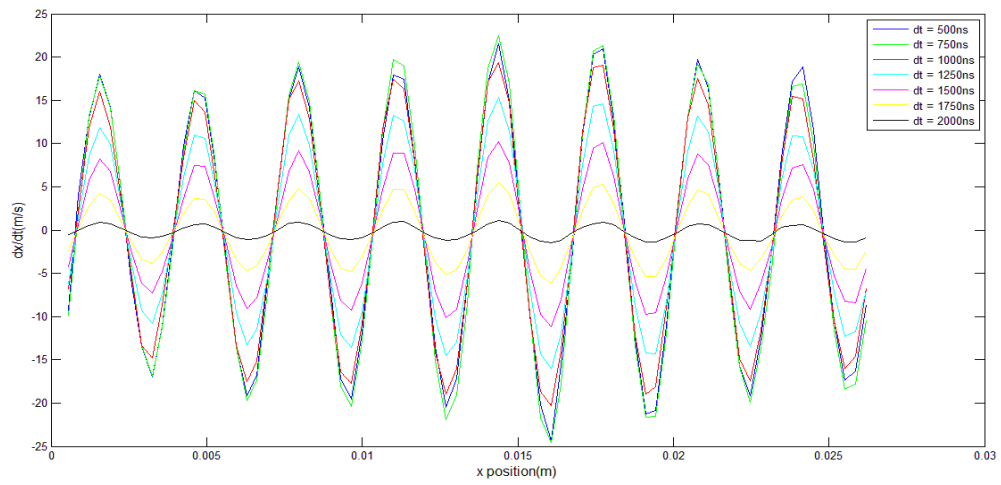
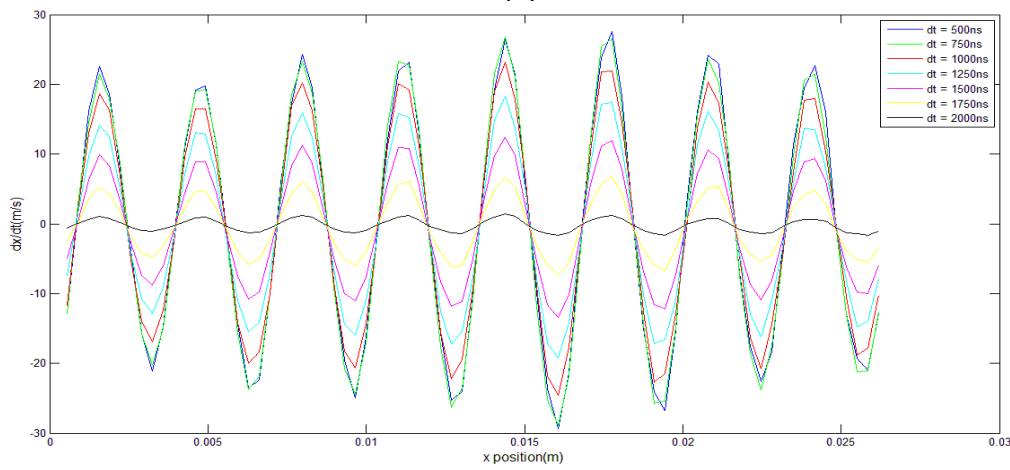


Figure 6 Displacement vector at different inter-frame time (time is in nsec)

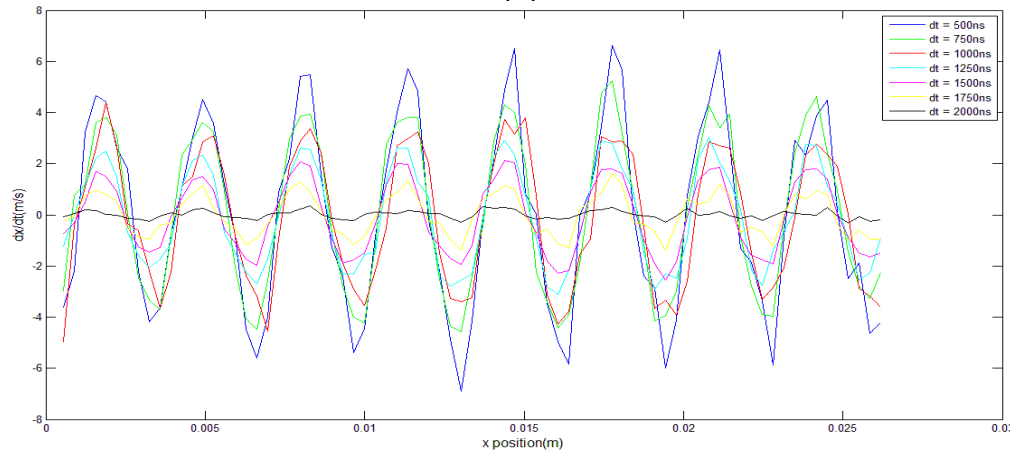
The effect of changing the intensity of the HIFU is shown in figure 7. Figure 7.a represents the velocity vector when the function generator is set to 1Vpp. Similarly, Figure 4.b represents the velocity vector when the function generator supplies 4Vpp .The difference between the two vectors is shown in figure 7.c. These results indicate that it is possible to correlate the obtained acoustic particle velocity with the intensity of the HIFU since the intensity of the latter changes proportionally with the applied voltage.



(a)



(b)



(c)

Figure 7: dx/dt vector at different inter-frame timings when the amplifier supplies its maximum amplification and the function generator supplies (a) 1Vpp (b) 4Vpp (c) the difference between them.

C. Conclusions from the Preliminary Experiment

For two different input powers, the higher electrical input power results in higher acoustic particle velocity measurements.

- 1- In this typical PIV procedure, the particle velocity is dependent on the chosen inter frame time; none of the results can be considered as actual particle velocity. So, alternative procedure must be performed to measure the actual velocity.
- 2- The maximum displacement occurred when the inter-frame time τ is around 1000 ns (half the wavelength).

CHAPTER IV

PROPOSED PROCEDURE

A. Procedure Description

The proposed procedure is illustrated in figure 8; the first PIV was executed using pictures captured at $t=T$ & $t=T+dt$, the second PIV was performed using pictures captured at $t=T$ & $t=T+dt+\tau$, the difference of the displacement between the two PIV represents the displacement of the particle during the time between $t=T+dt$ & $t=T+dt+\tau$, if we divide this displacement over τ the result will be the velocity at $t=T+dt+(\tau/2)$. In this work, the combination of these two PIV's will be called PIV block, dt will be called initial inter-frame time, and τ will be called increment time.

The block is repeated with the shift of τ in each time. Each time-block will assign one velocity for each point in the space. Then, the RMS value will be calculated in each point in the space using the assigned velocity values with the time.

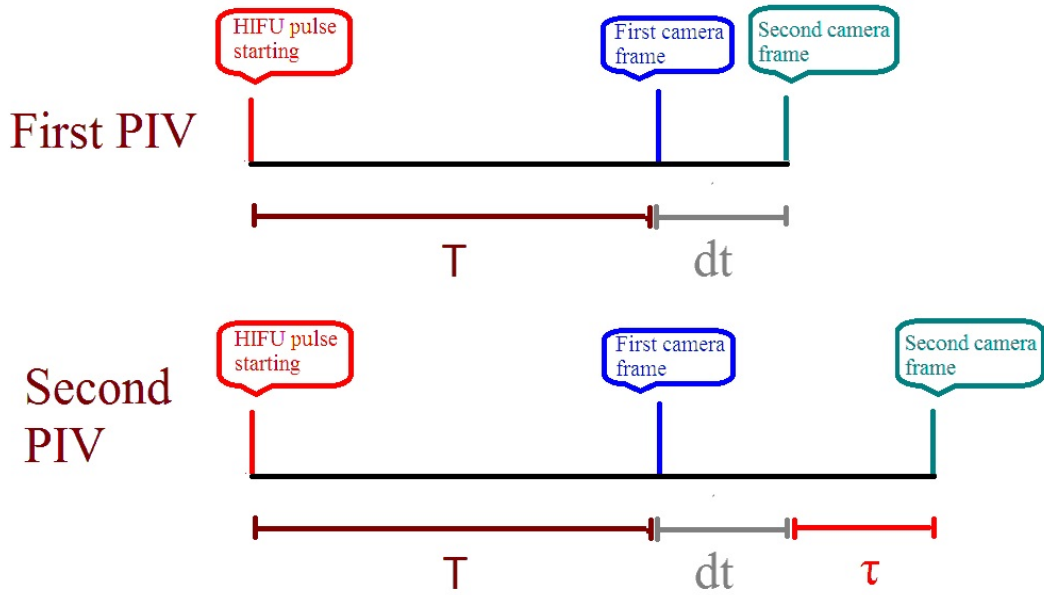


Figure 8: Time block for the proposed experiment

B. Matlab Simulation

To predict the results of the proposed procedure, Matlab simulation for the particles movement and the PIV procedure was performed. The particle displacement wave function was built using the following equation.

$$y(x, t) = 2 * 10^{-5} * \sin\left(\frac{2\pi}{\lambda} x - 2\pi f t\right)$$

$$f = 500 \text{ KHz}, \lambda = 3 \text{ mm}$$

First, the sensitivity of the selected increment time (τ) was measured depending on the resulting RMS-velocity value at one point. The results show that an increment time up to 200ns is recommended.

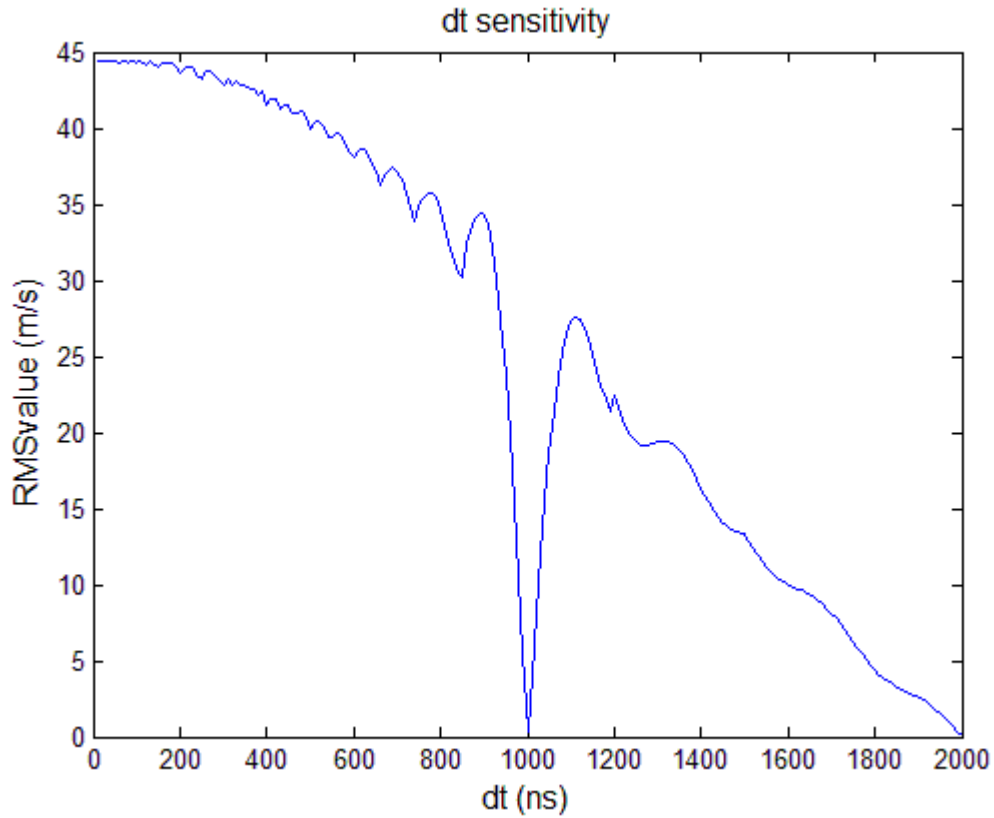


Figure 9: Sensitivity of the RMS- velocity value with the increment time

If we choose increment time (τ) of 100 ns, 20 PIV blocks are required to build a complete time- velocity profile at each point in the field. The simulation of the expected velocity fields at three different times is shown in figure 10, each of them represent a sample of the expected direct results of one horizontal line in the camera frame when one PIV block is performed.

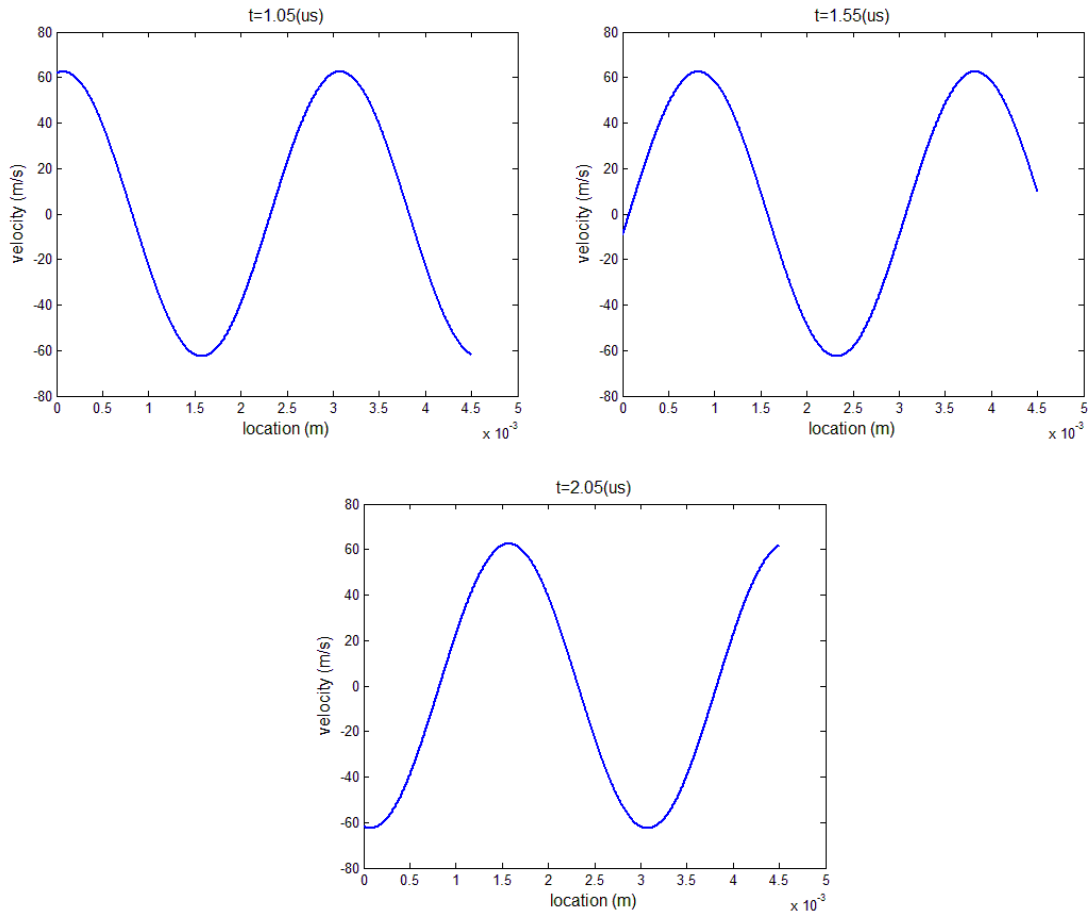


Figure 10: velocity fields resulted from Matlab simulation of PIV blocks procedure at three different times, $\tau=100$ ns

If we want to re-build the time-velocity profile at one point in space, the results are shown in the figure 11 for three different points. The re-building was done by relating each velocity value for the specified point from the required 20 PIV blocks with the time of $(T+dt+\tau/2)$ of the associated block. After re-building the velocity vector cycle at each point, RMS-velocity value can be calculated at each point in space as shown in figure 12. The RMS values are approximately the same at all points in the field because the difference between the velocity vectors at different points is only the starting phase.

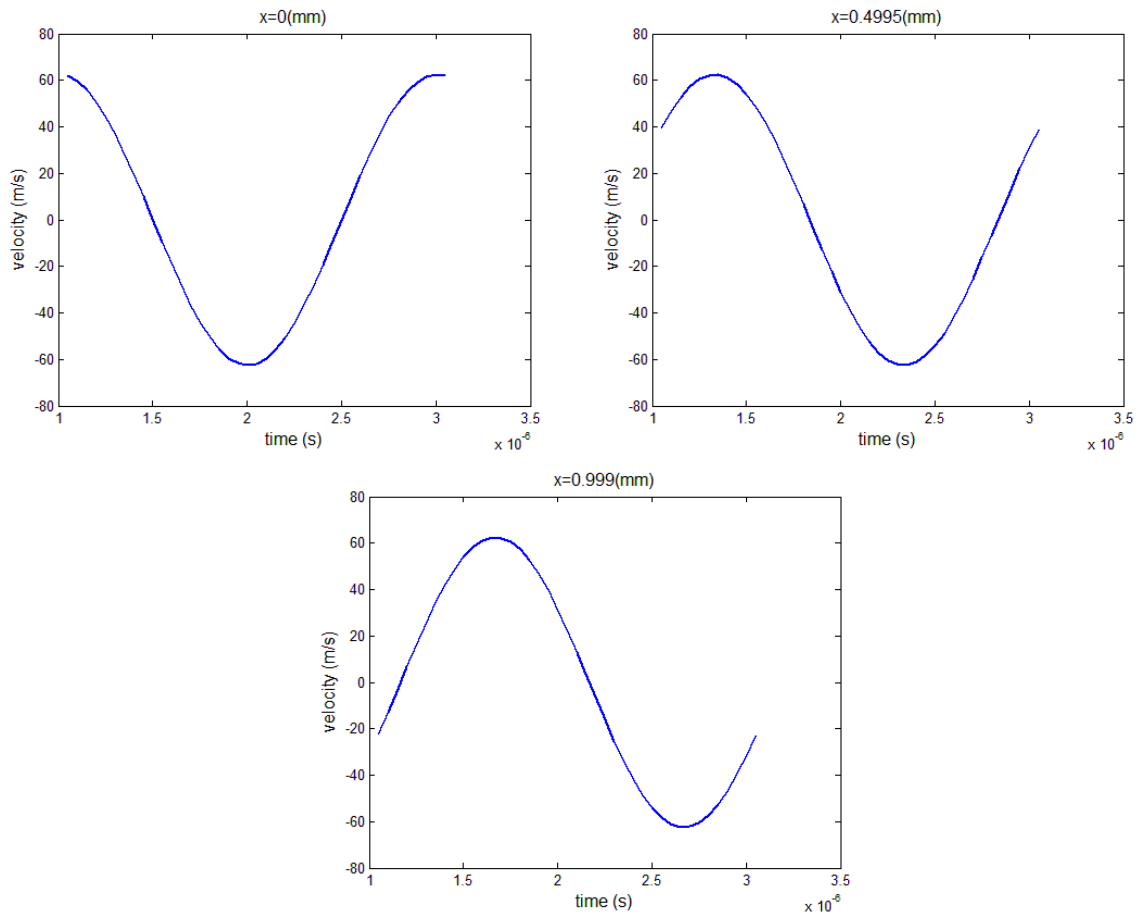


Figure 11: The expected time-velocity profile at three different points in the field resulting from Matlab simulation

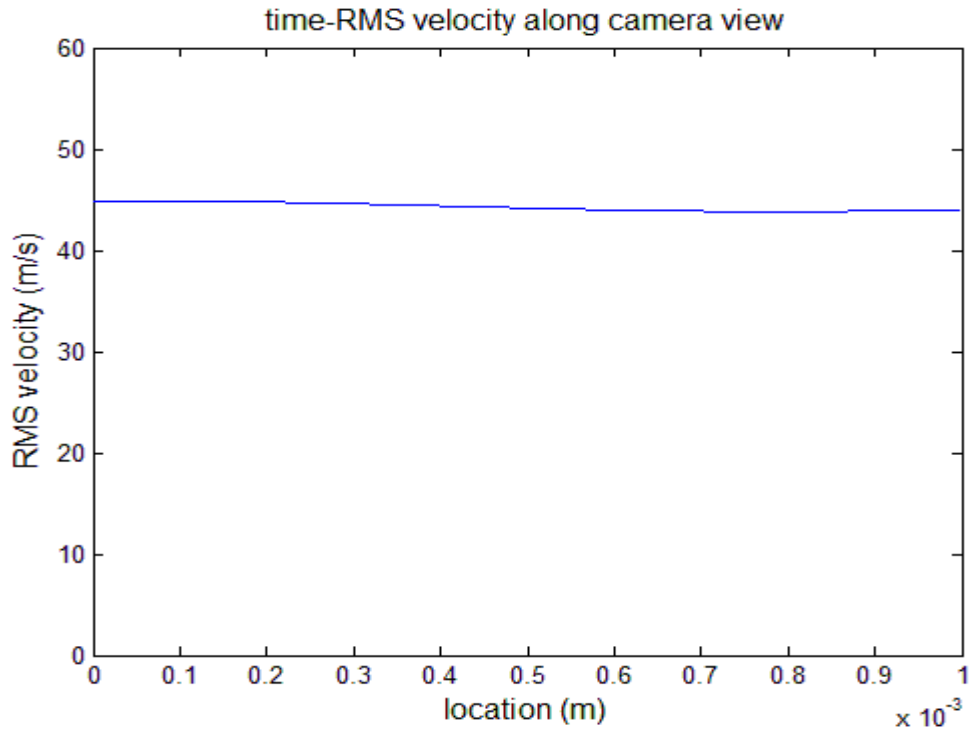


Figure 12: The RMS-velocity field resulted from Matlab simulation.

C. Real-World Experiment

In This experiment a water-nanoparticles vial was placed at the focal point. The time scheme for block procedure described in figure 8 was followed. For simplicity, the time of the first frame of the first PIV set was considered to be taken at $t=0$; this means that the HIFU burst was started at $t=-T$. the initial inter-frame time (dt) was chosen to be 1000 ns to get benefit from the maximum possible displacement, while the increment time (τ) was chosen to be 100ns depending on the sensitivity measurement in Matlab simulation (figure 9).

With increment time of 100 ns, 42 different PIV sets were required to cover a complete velocity cycle providing 21 PIV blocks. Where Set 1 and Set 2 formed the first block, Set 3 and Set 4 formed the second block and so on. Each block assigned one velocity value at each point in the field. The time for all the sets is shown in the table in appendix 1. The procedure is more explained in the figure 13 that describes the time scheme for the first and second PIV blocks. The first frame for both Set 1 and Set 2 were taken at $t=0$, while the second frame for them were taken at $t= 1000$ ns and $t= 1100$ ns respectively. The difference between the displacement fields resulting from them were used to calculate the velocity field at $t=1050$. The whole process was shifted by 100 ns in Set 3 and Set 4 to produce the second velocity field at $t=1150$. This procedure were repeated until getting the 21th velocity field at $t=3050$ using Set 41 and Set 42. This covered the whole acoustic velocity cycle.

Each set consists of 50 pairs with the same HIFU power and PIV timing. After processing the 50 pairs using PIV Matlab code and taking the average of them, the average field of that set was obtained. The average fields for the first and second sets are shown in figure 14.a&b. Figure 14.c shows the velocity field at $t= 1050$ which was produced using the difference field between the average fields of Set 1 and Set 2.

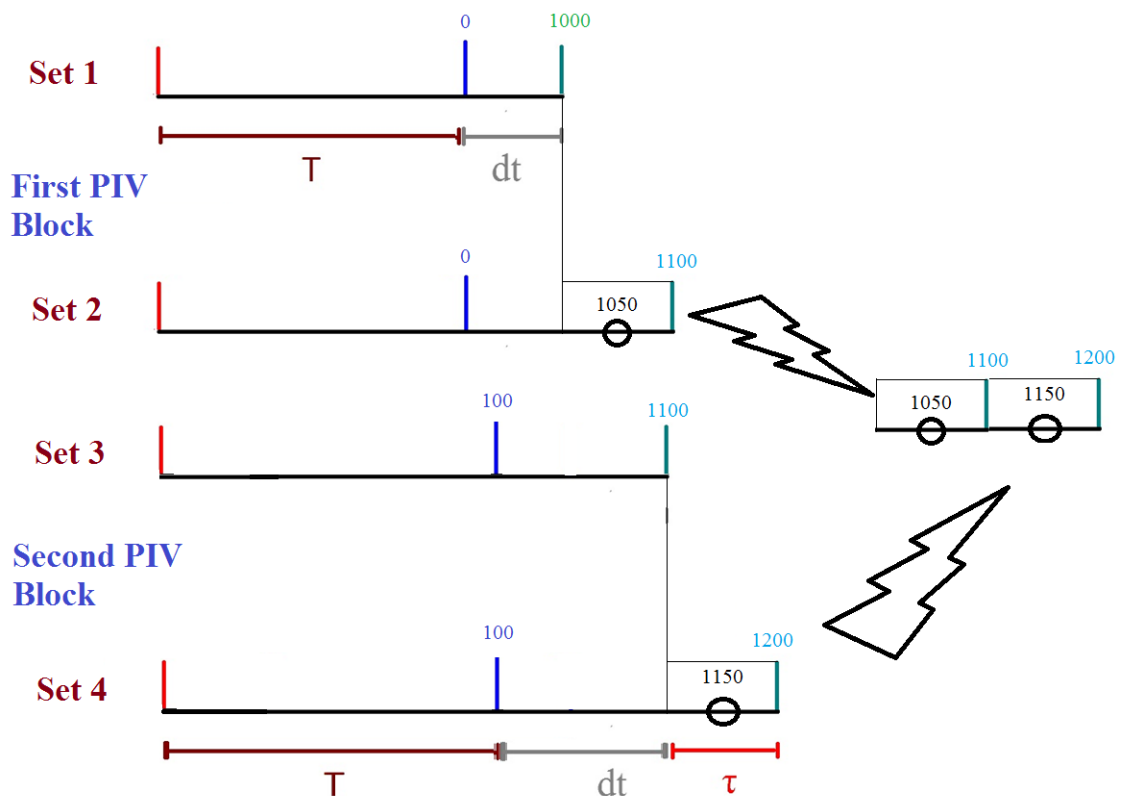


Figure 13: Time scheme of first and second PIV blocks

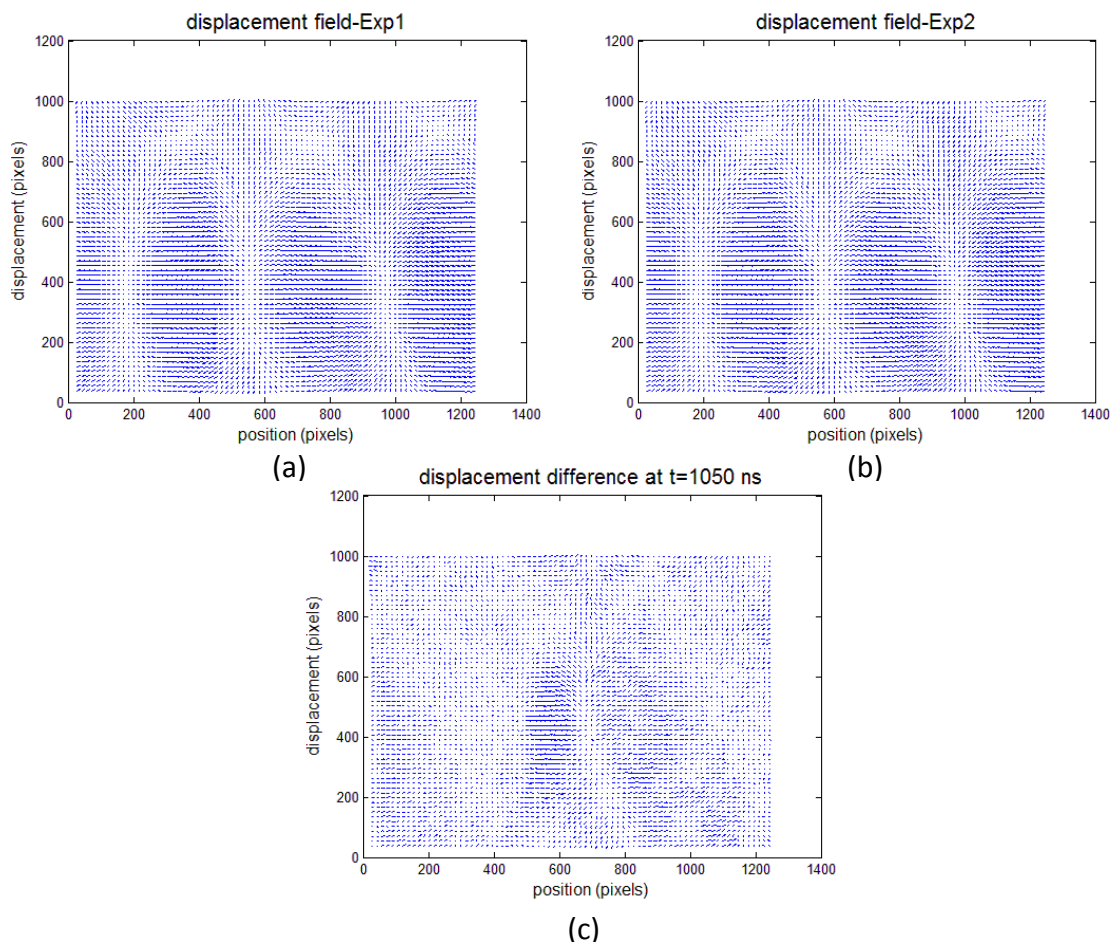


Figure 14: first PIV block fields; (a) the average displacement field for set 1, (a) the average displacement field for set 2, (c) the displacement field for PIV block 1.

At this stage, each point in the field became having 21 velocity values at time varying from $t=1050$ ns to $t=3050$ ns with increment of 100 ns. By relate each velocity value with its associated time; the time-velocity profile was obtained. Figure 15 visualizes the time-velocity profile at three points in the field. By comparing figure 11 and figure 15, it is clear that the obtained results are different from the expected ones.

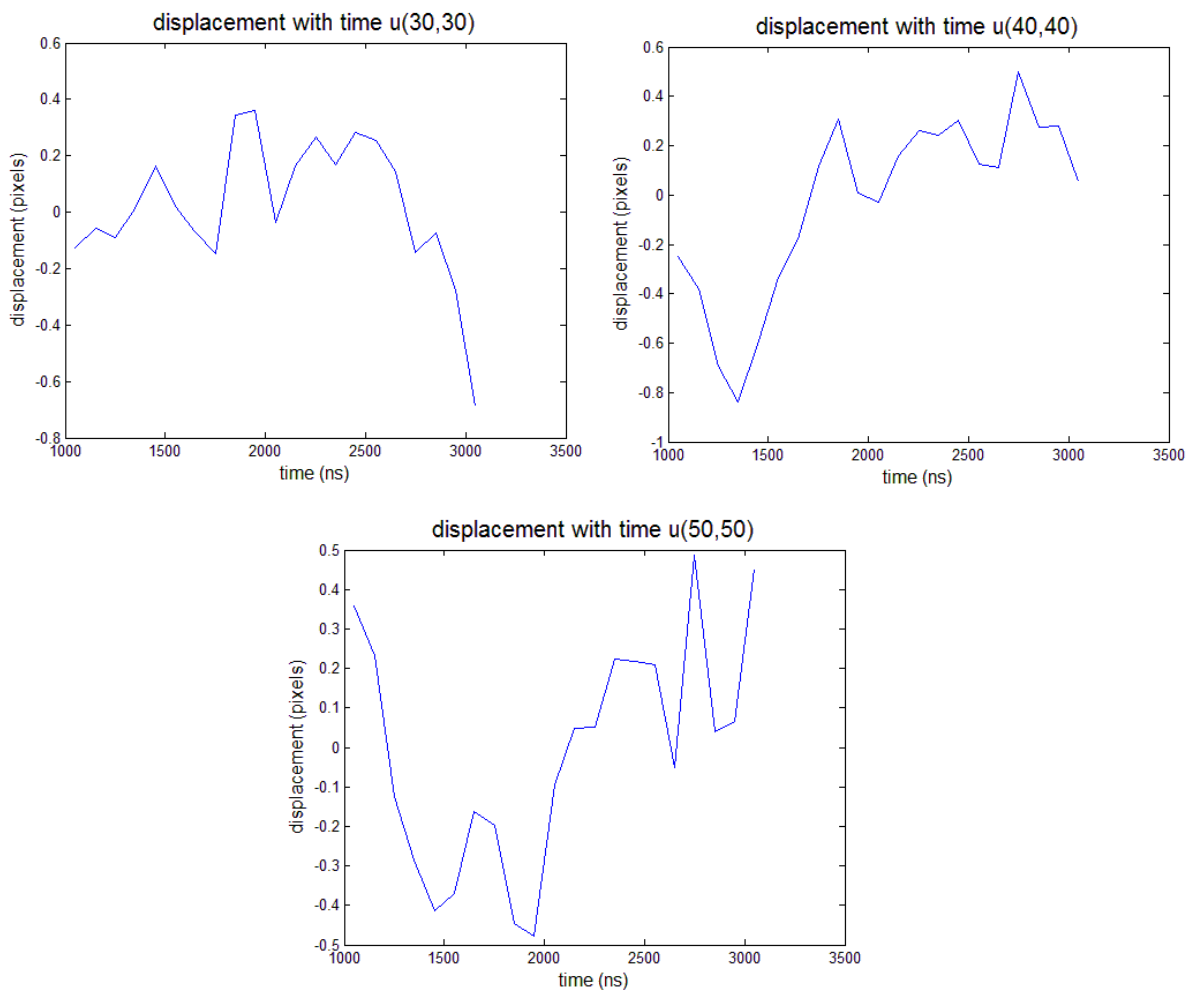


Figure 15: time-velocity profile at three points in the field

The RMS average value was calculated from the 21 time-velocity data points at each point in the field. The result is a field that represents the time-average velocity field, which is shown in figure 19, instead of instantaneous velocity field. Referring to figure 12, it was expected to have constant time RMS velocity a long any longitudinal axis in the field. Again, the obtained results differ from the expected one.

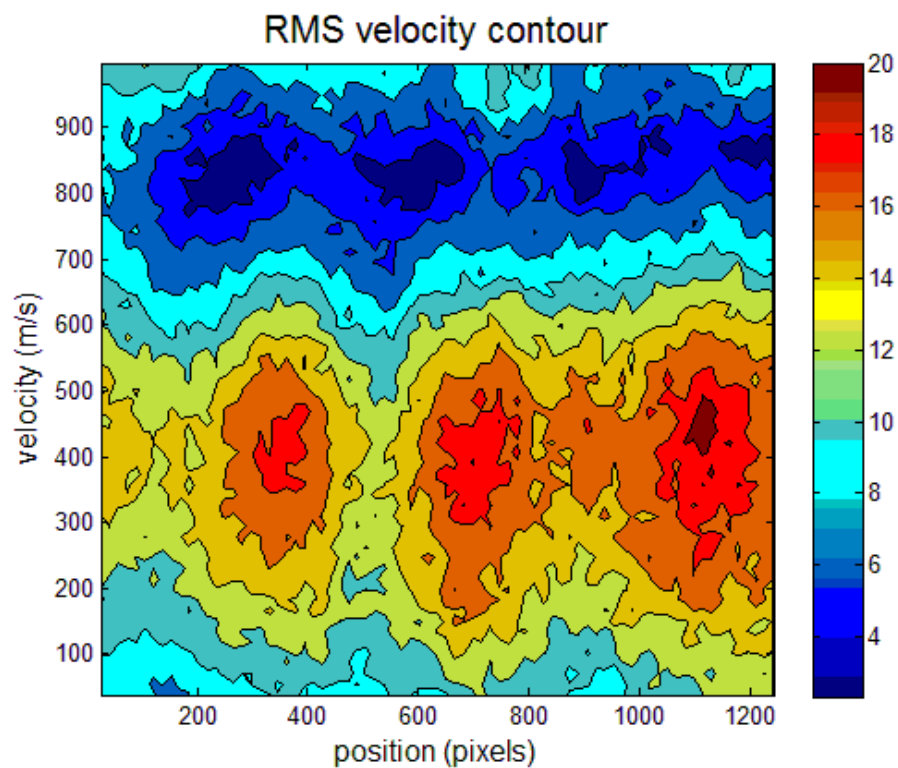


Figure 16: time RMS average velocity field at focal point resulted from applying PIV block technique

The difference between the expected and the obtained results was due to the existence of *Acousto-Optical Effect* in the HIFU field. Acousto-optical effect is a virtual particle deformation and displacement seen by the camera under the effect of the periodic region of

compression and refraction in a fluid that is subjected to a high intensity sound field like the HIFU.

CHAPTER V

ACOUSTO-OPTICS MEASUREMENT TECHNIQUE

A. Procedure Description

It is shown from the previous experiment that what was appeared as particles' movements have a component of virtual displacement due to the acousto-optical effect. This effect was seen to be dependable on the HIFU power and its contribution on the PIV results was greater than the contribution of actual particle displacement itself. This led to the idea of use this effect to calibrate the HIFU transducer.

In This experiment, a grid paper was placed at a location that witness high acousto-optical effect. Under the effect of HIFU power, grids appeared at the camera at shapes and sizes different from the real ones, this effect is shown at figure 17. Under the effect of HIFU bursts, pairs of images were taken and processed using PIV Matlab code. The change in grids' size and shape were appeared as particle movements which produced displacement fields.

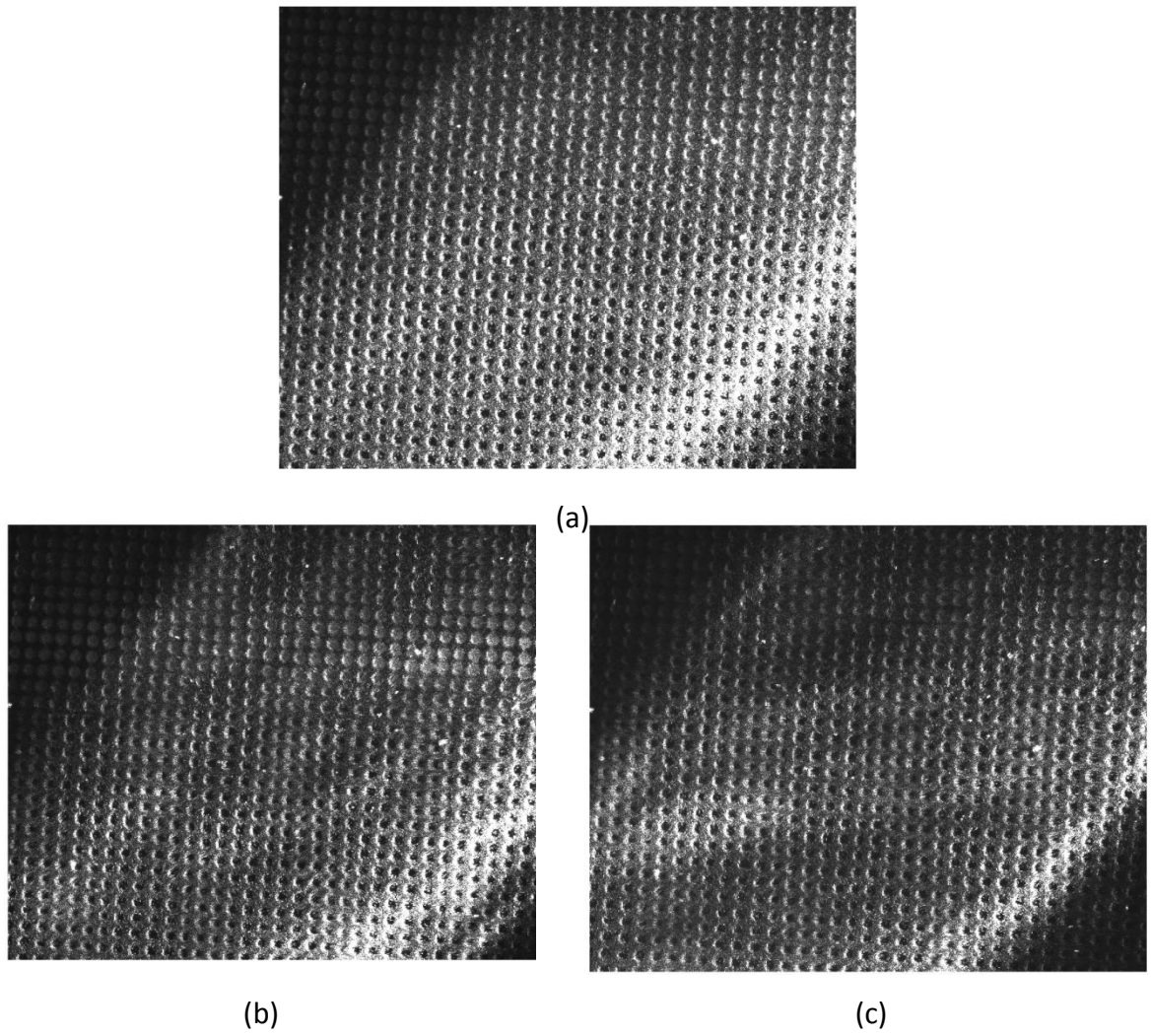


Figure 17: Acousto-optical effect as appears on capturing pictures for grid paper placed at HIFU field

B. Distance Effect

The first step was applying the technique at different distances from the HIFU axis. The grid paper and the laser sheet were moved by steps of 1 mm in the transverse direction closer and farther from the camera. 100 pairs of images were taken at each distance with HIFU acoustic intensity of 286 W/cm^2 and inter-frame time of 1000 ns. The distances were normalized by dividing them by the radius of the HIFU beam at the focal point. From the resulting velocity fields, the spatial RMS average of the velocity vectors along the HIFU center longitudinal axis and the parallel axes to it were calculated.

The effect of changing the distance are shown in the figure 18, which represent the spatial averaged velocity distribution along the transverse direction around the HIFU focal spot at each distance.

The peak of this plot at each power increment represents the spatial RMS average velocity along HIFU axis around the focal point. By relate this value with the normalized distance from HIFU axis, the changing of the acousto-optics effect with distance can be predicted. This is shown at figure 19.

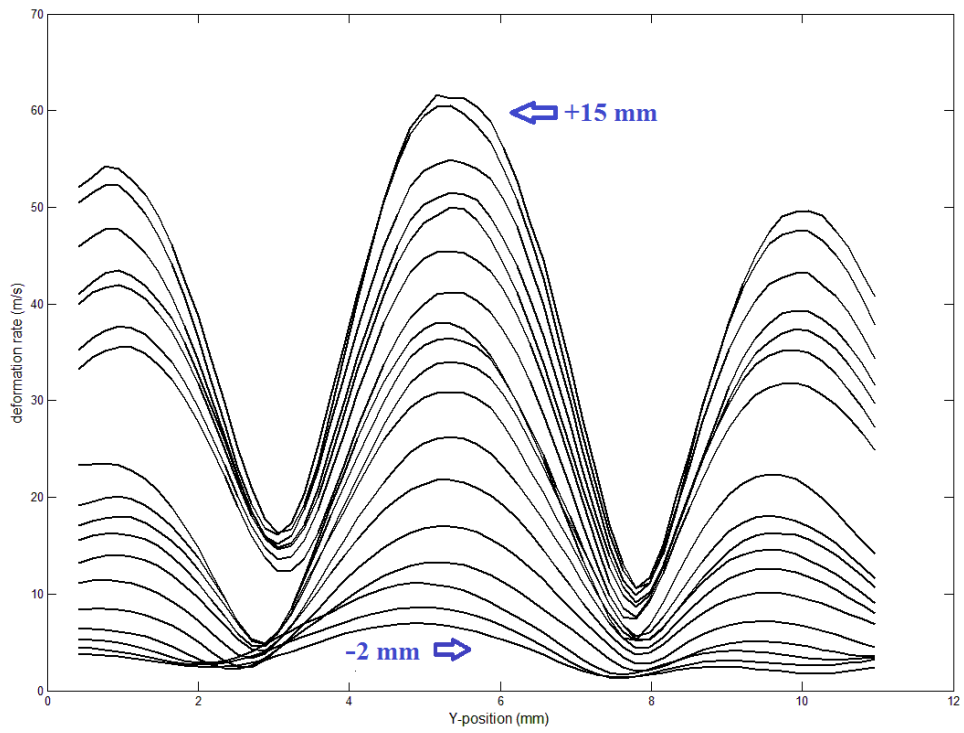


Figure 18: Spatial RMS average deformation rate of grids under the effect of HIFU field at different radial distances

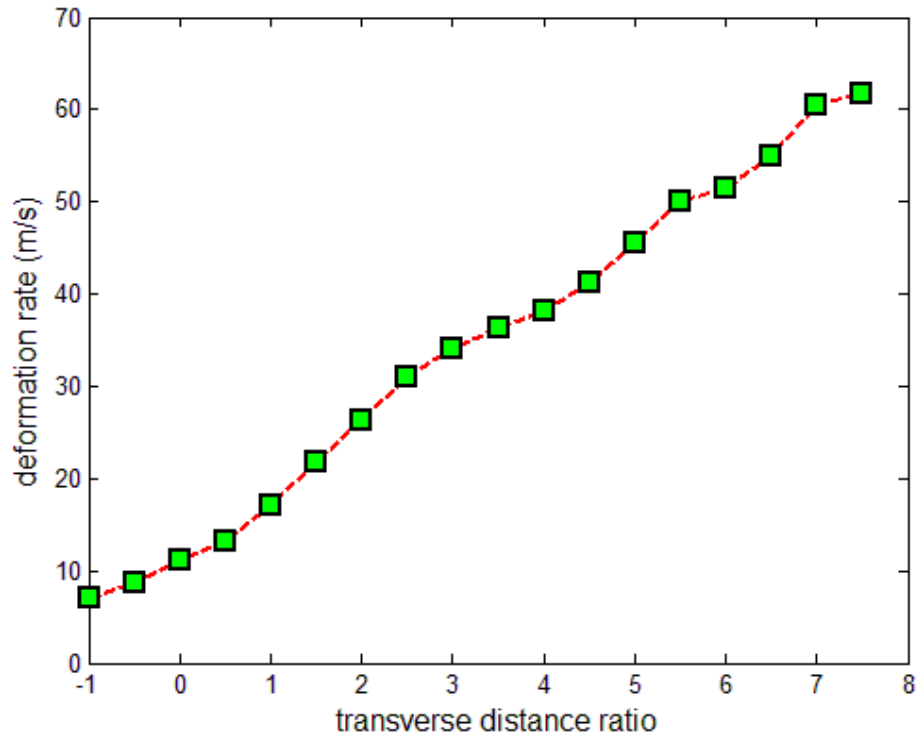


Figure 19: Changing of the acousto-optical effect with distance of grid sheet from the HIFU axis

C. Input Power Effect

After measuring the effect of the grid paper location with respect to the HIFU axis and the camera, there was a need to determine the effect of changing the HIFU power on the intensity of acousto-apical effect. To execute that, five different input electrical powers were used ranging from 3-48 W. They were measured using a wattmeter (MODEL 21A-Sonic Concept). Figure 3 were used to convert them into acoustic powers. These powers were divided by the cross section area for the HIFU beam at the focal point. This cross section area was determined depending on the manufacturer measurements.

At each acoustic intensity increment, 11 different PIV sets were taken. Each set consists of 50 pairs of images at the same power and timing to take the average of them.

The time of the first frame at all the sets was constant, while the second frame time differed. For simplicity and referencing, we consider that the first frame was taken at $t=0$. The timing of the 11 sets is shown at the following table.

The difference between each two consecutive sets was obtained. After dividing the difference on the time difference between the inter frame time, the deformation rate was obtained and placed at t Where

$$t = \frac{\text{SecondPIVSecondFrameTime} - \text{FirstPIVSecondFrameTime}}{2} + \text{FirstPIVSecondFrameTime}$$

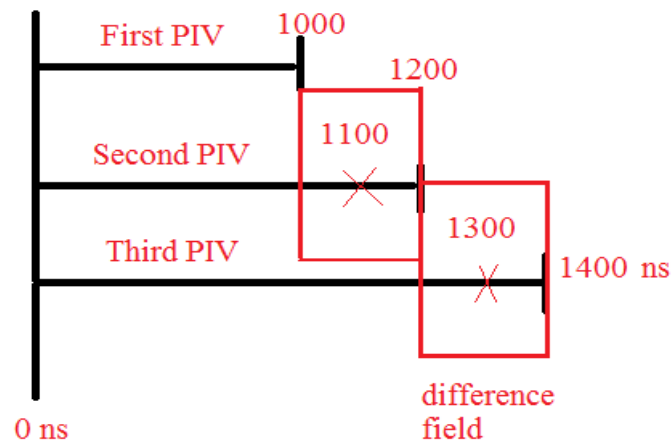


Figure 20: Time scheme for acousto-optical experiment

At this stage, each point in the field became having 11 deformation rate values at time varying from $t=1100$ ns to $t=2900$ ns with increment of 200 ns. By relate each displacement value with its related time; the time-displacement profile was obtained. The RMS average value was calculated from the 11 time-deformation rate data points at each

point in the field. The results are shown in figure 21 and they represent the time-average deformation rate fields at five different powers.

After taking the time averaged RMS velocity at each point in the field which produced time-averaged fields, another RMS average could be taken, which is this time spatial average. This was performed by calculating the RMS average of the velocity vectors along the HIFU center longitudinal axis and the parallel axes to it from the time- averaged field. This produced time and spatial averaged velocity distribution along the transverse direction around the HIFU focal spot.

The peak of this plot at each power increment represents the time-spatial RMS average deformation rate along HIFU axis around the focal point. By relate this value for the acoustic intensity, depending on the manufacturer calibration, the figure 23 was produced. This figure can be used to predict the acoustic power at other measured averaged acoustic velocity.

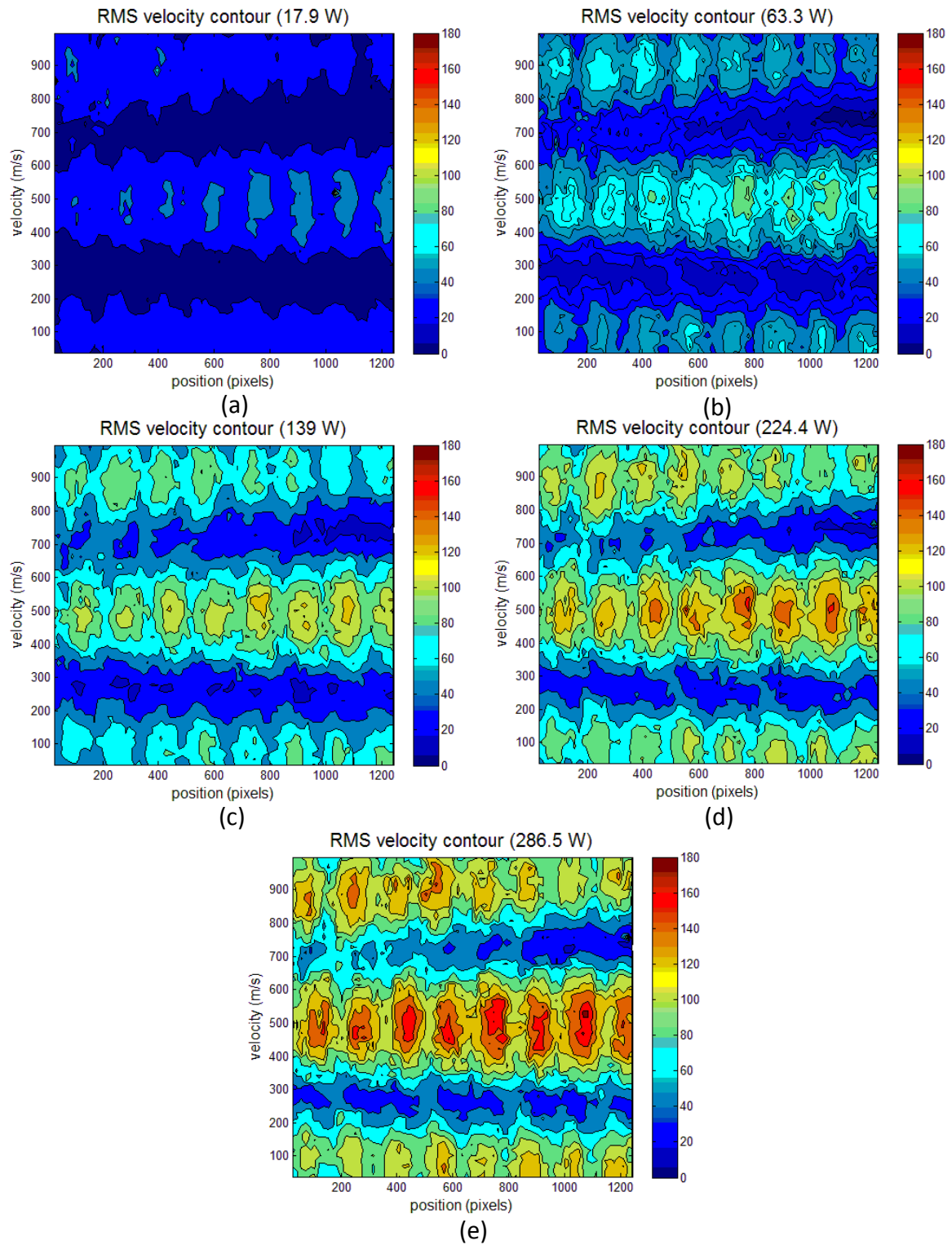


Figure 21: the time-average deformation rate fields at five different powers

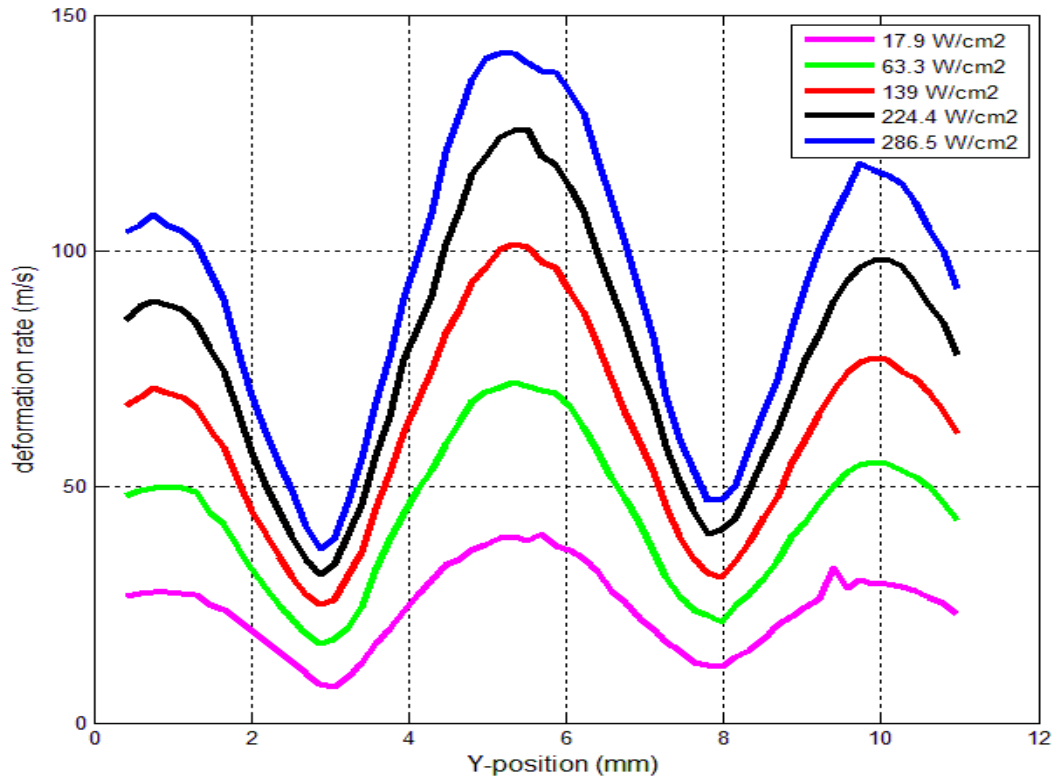


Figure 22: Time and spatial averaged velocity distribution along the transverse direction around the HIFU focal spot

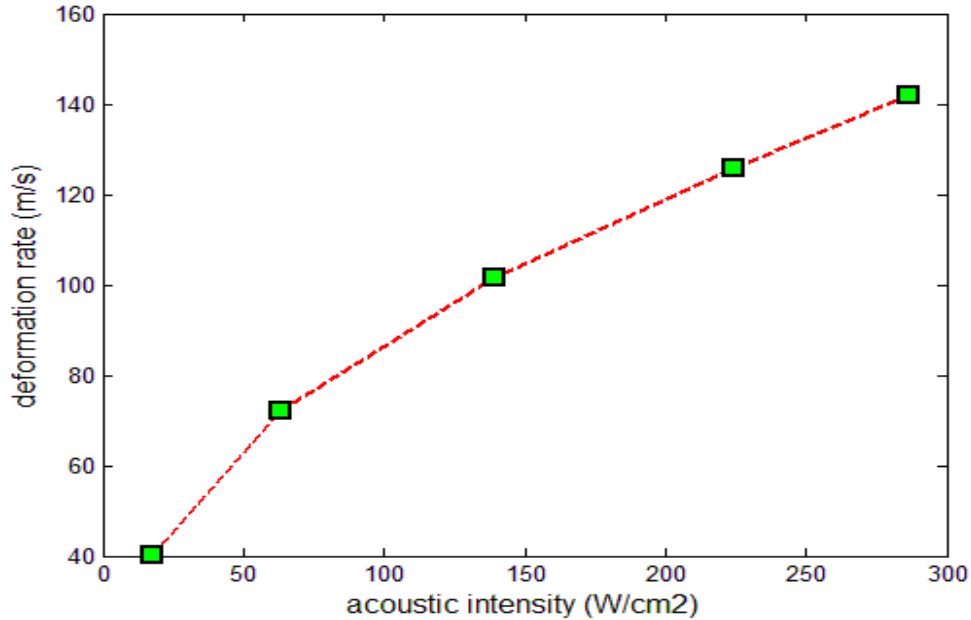


Figure 23: The change of the time-spatial RMS average deformation rate along HIFU axis with the change of acoustic intensity

D. Proposed Calibration Procedure

Depending on the results, the acousto-optics effect can be used to calibrate the HIFU transducer using these steps:

- 1- A water- nanoparticles vial will be located at the focal region and perform a typical PIV measure on it with inter-frame time equal to half the wavelength of the used HIFU transducer. From the results, the focal width of the HIFU beam at the focal spot can be determined.
- 2- A grid sheet will be located behind the foal region in the transverse direction (the focal region to be between the camera and the grid paper). By doing this, the HIF_field will not be interrupted by the sheet. The distance of grid paper from the HIFU axis will be normalized over the half of the focal width.

- 3- (ACOUSTO-OPTICS MEASUREMENT TECHNIQUE) described in this chapter, will be followed. At least 10 deformation rate measurements will be needed within a time of one HIFU cycle. The time- RMS average deformation rate field, then, will be calculated. From this field, spatial RMS average along the HIFU longitudinal axis will be calculated. Figure 23 will be used to get the HIFU acoustic intensity. If the normalized distance other than 5.5 would be used, figure 19 can be used to compensate the difference.
- 4- Step three will be repeated at different input electrical power and the electrical power will be measured. From the acoustic intensity resulted from step 3 and focal width measured from step 2, acoustic power can be measured.
- 5- By relate the input electrical powers used and the resulting acoustic power, the HIFU transducer efficiency curve, similar to figure 3, can be obtained.

CHAPTER VI

CONCLUSION

Typical PIV procedure was used to configure the HIFU field in a water bath. It was shown that the main limitation for that was the difficulty to reach inter-frame time small enough in comparison with the wavelength of the HIFU. However, it showed that an increase of input power results in increase in acoustic particle velocity.

To overcome the time problem, the PIV blocks procedure were proposed, but the non-linear effects associated with the HIFU field affected the results making them different from the expected ones. The most important effect was the acousto-optical effect. Theoretically, this procedure may be an appropriate tool to study other ultrasound applications that have lower acoustic intensity than the HIFU. However, this needs to be validated in future.

Instead of trying to eliminate the acousto-optical effect, the decision was made to use it as a proposed calibration tool for the HIFU transducers. For that reason, A PIV experiment was designed to measure the deformation of pictures captured for a grid sheet (virtual displacement) instead of measuring actual particle displacement. A novel procedure to calibrate the HIFU could be presented as a result of this experiment.

REFERENCES

- Azhari, H. (2010). Basics of biomedical ultrasound for engineers John Wiley & Sons.
- Berson, A., Michard, M., & Blanc-Benon, P. (2008). Measurement of acoustic velocity in the stack of a thermoacoustic refrigerator using particle image velocimetry. *Heat and Mass Transfer*, 44(8), 1015-1023.
- Bessonova, O. V., & Wilkens, V. (2013). Membrane hydrophone measurement and numerical simulation of HIFU fields up to developed shock regimes. *Ultrasonics, Ferroelectrics, and Frequency Control, IEEE Transactions on*, 60(2), 290-300.
- Campbell, M., Cosgrove, J., Greated, C., Jack, S., & Rockliff, D. (2000). Review of LDA and PIV applied to the measurement of sound and acoustic streaming. *Optics & Laser Technology*, 32(7), 629-639.
- Canney, M. S., Bailey, M. R., Crum, L. A., Khokhlova, V. A., & Sapozhnikov, O. A. (2008). Acoustic characterization of high intensity focused ultrasound fields: A combined measurement and modeling approach. *The Journal of the Acoustical Society of America*, 124(4), 2406-2420.
- Curra, F. P., & Crum, L. A. (2003). Therapeutic ultrasound: Surgery and drug delivery. *Acoustical Science and Technology*, 24(6), 343-348.
- Fischer, A., Sauvage, E., & Roehle, I. (2008). Acoustic PIV: Measurement of the acoustic particle velocity using synchronized PIV-technique. *The Journal of the Acoustical Society of America*, 123(5), 3130. doi:10.1121/1.2933079
- Han, D., & Mungal, M. (2003). Simultaneous measurements of velocity and CH distributions. part 1: Jet flames in co-flow. *Combustion and Flame*, 132(3), 565-590.
- Hann, D., & Greated, C. (1997). Particle image velocimetry for the measurement of mean and acoustic particle velocities. *Measurement Science and Technology*, 8(6), 656.
- Hann, D., & Greated, C. (1997). Particle image velocimetry for the measurement of mean and acoustic particle velocities. *Measurement Science and Technology*, 8(6), 656.
- Hariharan, P., Myers, M. R., Robinson, R. A., Maruvada, S. H., Sliwa, J., & Banerjee, R. K. (2008). Characterization of high intensity focused ultrasound transducers using acoustic streaming. *The Journal of the Acoustical Society of America*, 123(3), 1706-1719.
- Humphreys, W. M., Bartram, S. M., Parrott, T. L., & Jones, M. G. (1998). Digital piv measurements of acoustic particle displacements in a normal incidence impedance tube. 20th AIAA Advanced Measurement and Ground Testing Technology Conference, 15-18.
- Nabavi, M., Siddiqui, M. K., & Dargahi, J. (2007). Simultaneous measurement of acoustic and streaming velocities using synchronized PIV technique. *Measurement Science and Technology*, 18(7), 1811.
- Quraini, M. M. (2012). Experiments on the Heating and Mechanical Effects of High Intensity Focused Ultrasound,

- Rockliff, D. (2002). Application of Particle Image Velocimetry to the Measurement of Non-Linear Effects Generated by High-Intensity Acoustic Fields,
- Shaw, A., Khokhlova, V., Bobkova, S., Gavrilov, L., & Hand, J. (2011). Calibration of HIFU intensity fields measured using an infra-red camera. *Journal of Physics: Conference Series*, , 279(1) 012019.
- Shaw, A., & Hodnett, M. (2008). Calibration and measurement issues for therapeutic ultrasound. *Ultrasonics*, 48(4), 234-252.
- ter Haar, G. (2007). Therapeutic applications of ultrasound. *Progress in Biophysics and Molecular Biology*, 93(1–3), 111-129. doi:<http://dx.doi.org/10.1016/j.pbiomolbio.2006.07.005>
- Tonndast-Navæi, A. (2004). Acoustic Particle-Image Velocimetry: Development and Applications,
- Tonndast-Navæi, A. (2006). Acoustic particle-image velocimetry: Development and applications
- Van Der Eerden, F., De Bree, H., & Tjeldeman, H. (1998). Experiments with a new acoustic particle velocity sensor in an impedance tube. *Sensors and Actuators A: Physical*, 69(2), 126-133.
- Zhou, Y. F. (2011). High intensity focused ultrasound in clinical tumor ablation. *World Journal of Clinical Oncology*, 2(1), 8-27. doi:10.5306/wjco.v2.i1.8 [doi]

APPENDIX 1

TIME SCHEME FOR PIV SETS IN THE PIV BLOCKS EXPERIMENT

Set#	First Frame time (ns)	Second Frame time (ns)
Set 1	0	1000
Set 2	0	1100
Set 3	100	1100
Set 4	100	1200
Set 5	200	1200
Set 6	200	1300
Set 7	300	1300
Set 8	300	1400
Set 9	400	1400
Set 10	400	1500
Set 11	500	1500
Set 12	500	1600
Set 13	600	1600

Set 14	600	1700
Set 15	700	1700
Set 16	700	1800
Set 17	800	1800
Set 18	800	1900
Set 19	900	1900
Set 20	900	2000
Set 21	1000	2000
Set 22	1000	2100
Set 23	1100	2100
Set 24	1100	2200
Set 25	1200	2200
Set 26	1200	2300
Set 27	1300	2300
Set 28	1300	2400
Set 29	1400	2400
Set 30	1400	2500
Set 31	1500	2500

Set 32	1500	2600
Set 33	1600	2600
Set 34	1600	2700
Set 35	1700	2700
Set 36	1700	2800
Set 37	1800	2800
Set 38	1800	2900
Set 39	1900	2900
Set 40	1900	3000
Set 41	2000	3000
Set 42	2000	3100

APPENDIX 2

TIME SCHEME FOR PIV SETS IN THE ACOUSTO-OPTICAL EXPERIMENT

Set#	First Frame time (ns)	Second Frame time (ns)
Set 1	0	1000
Set 2	0	1200
Set 3	0	1400
Set 4	0	1600
Set 5	0	1800
Set 6	0	2000
Set 7	0	2200
Set 8	0	2400
Set 9	0	2600
Set 10	0	2800
Set 11	0	3000

